

Figure 1. Thermogram of $\text{Mo}_2(\text{O-cy-C}_6\text{H}_{11})_6$ under He flow (50 mL/min) showing the weight loss versus temperature profile with a heating rate of $10\text{ }^\circ\text{C}/\text{min}$.

train and oxygen analyzer. The atmosphere in the box was chosen to be He (less than 1 ppm O_2) so as to eliminate the problems arising from static electricity. Under these rigorous conditions $\text{Al}_2(\text{O-}t\text{-Bu})_6$ sublimes without decomposition at ca. $200\text{--}220\text{ }^\circ\text{C}$, 1 atm. However, in the presence of trace amounts of moisture or oxygen, i.e., when the He carrier gas is not purified or when the TGA-MS is performed "outside" of the drybox using a glovebag and N_2 purge for sample preparation, the $\text{M}_2(\text{O-}t\text{-Bu})_6$ compounds where $\text{M} = \text{Al}$ and Mo decompose in the temperature range $190\text{--}230\text{ }^\circ\text{C}$ to give $\gamma\text{-Al}_2\text{O}_3$ and MoO_2 , respectively. The volatile components were $t\text{-BuOH}$, $\text{Me}_2\text{C}=\text{CH}_2$, and $t\text{-BuH}$. Under the more rigorous conditions, $\text{Mo}_2(\text{O-}t\text{-Bu})_6$ undergoes competitive sublimation and decomposition to yield MoO_2 at ca. $200\text{ }^\circ\text{C}$.

By contrast $\text{Mo}_2(\text{O-cy-C}_6\text{H}_{11})_6$ undergoes thermolysis in two distinct stages as shown in Figure 1. At around $210\text{ }^\circ\text{C}$ there is elimination of cyclohexane, cyclohexene, cyclohexanone, and cyclohexanol to give a material of composition $\text{Mo}_2\text{C}_4\text{O}_4$ that is stable to $550\text{ }^\circ\text{C}$. This material shows a diffuse X-ray diffraction pattern that is consistent with very fine grains (on the order of 20 \AA) of $\gamma\text{-MoC}$ suspended in an amorphous matrix. When this is heated to $660\text{--}706\text{ }^\circ\text{C}$, carbon dioxide and carbon monoxide are evolved according to the stoichiometry $\text{Mo}_2\text{C}_4\text{O}_4 \rightarrow \gamma\text{-Mo}_2\text{C} + \text{CO}_2 + 2\text{CO}$. The carbide $\gamma\text{-Mo}_2\text{C}$ was identified by elemental composition and X-ray diffraction (XRD).

It is known from previous work that $\text{W}_2(\text{OR})_6$ compounds are less thermally stable than their molybdenum analogues.⁷ None are known to sublime without decomposition. We find that $\text{W}_2(\text{O-}t\text{-Bu})_6$ is cleanly converted to WO_2 (elemental composition, XRD) at $120\text{--}200\text{ }^\circ\text{C}$ even under the most rigorously pure He atmosphere. The cyclohexoxide $\text{W}_2(\text{O-cy-C}_6\text{H}_{11})_6$ undergoes a decomposition that is superficially similar to its molybdenum analogue. When this is heated to $200\text{--}250\text{ }^\circ\text{C}$, cyclohexane, cyclohexene, cyclohexanone, and cyclohexanol are evolved with the formation of a material of composition $\text{W}_2\text{C}_4\text{O}_4$ that is thermally stable to $750\text{ }^\circ\text{C}$. However, at ca. $800\text{ }^\circ\text{C}$, this material evolves carbon monoxide, yielding tungsten metal (XRD) with only trace detectable quantities of WO_2 (XRD) as shown in Figure 2.

The following points are worthy of note:

Trace quantities of H_2O (or O_2) may facilitate an autocatalytic decomposition as seen here for $\text{Mo}_2(\text{O-}t\text{-Bu})_6$ and $\text{Al}_2(\text{O-}t\text{-Bu})_6$. This type of autocatalytic decomposition was

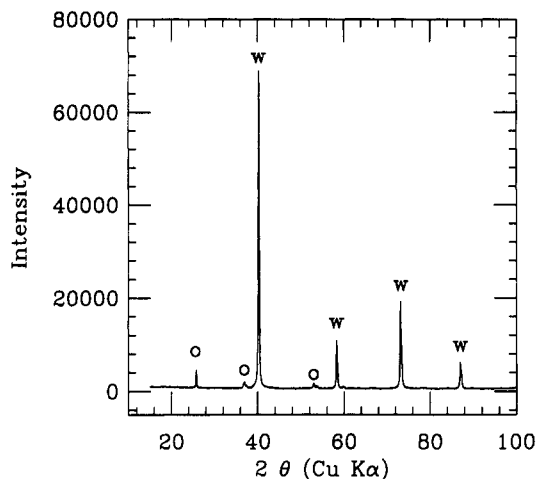


Figure 2. X-ray diffraction pattern on the ultimate product formed in the thermal decomposition of $\text{W}_2(\text{O-cy-C}_6\text{H}_{11})_6$ after heating to $1000\text{ }^\circ\text{C}$ under a He flow. The identifiable species are $\text{W}(\text{m})$ and WO_2 as shown by W and O in the figure.

first seen by Bradley and Factor^{3b} in their pioneering studies of the thermal decomposition of $\text{Zr}(\text{O-}t\text{-amyl})_4$.

The stoichiometry of the oxide M_2O_3 ($\text{M} = \text{Al}$) or MO_2 ($\text{M} = \text{Mo}$ and W) reflects the influence of the metal in achieving a thermodynamically stable oxide. There is no known oxide of formula W_2O_3 , and only recently has Mo_2O_3 been mentioned in the literature.⁸

The partitioning of products between MO_2 and Mo_2C or $\text{W}(\text{m})$ as a function of $\text{R} = t\text{-Bu}$ versus cy-Hex indicates the potential versatility of metal alkoxides as single source precursors and that much needs to be learned before product formation is predictable.

Acknowledgment. We thank the National Science Foundation for financial support of this work and Indiana Research and Development for the purchase of equipment.

(8) Babenko, V. I.; Grigoriev, S. M.; Utenkova, O. V.; Brazhevskii, V. P. Patent SU1469402A1, 1989; CA111(6):49601W.

Kinetic Studies of the Chemical Vapor Deposition of Platinum

Barbara Nixon, Peter R. Norton,* Eric C. Ou, Richard J. Puddephatt,* Sujit Roy, and Paul A. Young

Department of Chemistry
University of Western Ontario
London, Canada N6A 5B7

Received November 8, 1990
Revised Manuscript Received January 22, 1991

The organometallic chemical vapor deposition (CVD) of metallic platinum films has potential applications in microelectronics and in wear protection and has been the subject of several recent studies.¹⁻³ Qualitative observa-

(1) (a) Xue, Z.; Strouse, M. J.; Shuh, D. K.; Knobler, C. B.; Kaesz, H. D.; Hicks, R. F.; Williams, R. S. *J. Am. Chem. Soc.* 1989, 111, 8779. (b) Koplitz, L. V.; Shuh, D. K.; Chen, Y.-J.; Williams, R. S.; Zink, J. I. *Appl. Phys. Lett.* 1988, 53, 1705. (c) Chen, Y.-J.; Kaesz, H. D.; Thridandam, H.; Hicks, R. F. *Appl. Phys. Lett.* 1988, 53, 1591. (d) Gozum, J. E.; Pollina, D. M.; Jensen, J. A.; Giolami, G. S. *J. Am. Chem. Soc.* 1988, 110, 2688.

(7) Akiyama, M.; Chisholm, M. H.; Cotton, F. A.; Extine, M. W.; Haftko, D. A.; Little, D.; Fanwick, P. E. *Inorg. Chem.* 1979, 18, 2262.

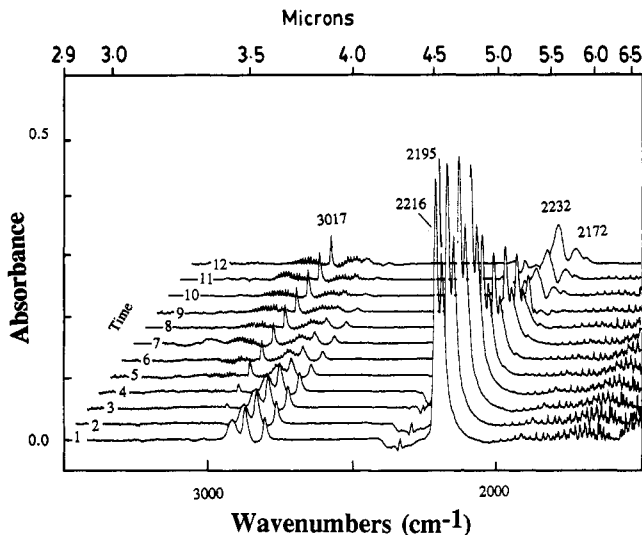


Figure 1. Stacked FTIR spectra recorded during the CVD of platinum from *cis*-[PtMe₂(MeNC)₂] at 250 °C. The growth of the peak due to methane [$\nu(\text{CH}) = 3017 \text{ cm}^{-1}$] and the decay of the stronger band due to the N≡C stretch of 1 [$\nu(\text{N}\equiv\text{C}) = 2216 \text{ cm}^{-1}$] were monitored with time. The latter was complicated by the growth of a broad band at 2232 cm⁻¹ due to a polymeric material.

tions with several precursors have indicated that CVD can be enhanced by the presence of H₂, by UV irradiation, and by other methods, but no kinetic studies of platinum CVD have been reported. This article describes the use of FTIR and UV spectroscopies to monitor the rate of CVD of platinum with *cis*-[PtMe₂(MeNC)₂], 1, as precursor.

Thermal CVD was monitored by FTIR using an evacuated 10-cm path length Pyrex cell, fitted with KCl windows. The cell was heated with electric tapes and insulated with aluminum foil. The tapes were arranged so that the windows, while hot, were at a temperature below the decomposition temperature, while the central part of the cell in which CVD occurred was at 250 °C. No deposition occurred on the windows, and continuous platinum films were formed in the central hot zone. The temperatures at several positions on the cell were monitored by using iron-constantin thermocouples. The products were methane [$\nu(\text{CH}) = 3017 \text{ cm}^{-1}$], platinum, and an involatile, insoluble oily polymer derived from the methyl isocyanide ligands that gave broad IR absorptions at 2232 and 2172 cm⁻¹ (Figure 1). Using the precursor *cis*-[Pt(CD₃)₂(MeNC)₂], 1', the volatile product of CVD was CD₃H [$\nu(\text{CD}) = 2291 \text{ cm}^{-1}$] with no CD₄ [$\nu(\text{CD}) = 2259 \text{ cm}^{-1}$] detectable. In a similar way the product of CVD from 1 in the presence of D₂ was shown to be CH₃D. The kinetics of CVD from *cis*-[PtMe₂(MeNC)₂] were studied by monitoring the appearance of methane or the disappearance of *cis*-[PtMe₂(MeNC)₂], which has $\nu(\text{N}\equiv\text{C}) = 2216$ and 2195 cm⁻¹ (Figure 1). Since several minutes were required to heat the cell to 250 °C, the kinetics of the earliest part of the reaction, where any induction period would be observed, could not be determined. The following are the major observations for CVD in the absence of UV light:

(1) In the absence of hydrogen, the rate of formation of methane or decay of complex 1 was first order in 1 with $k_{\text{obs}} = (6.0 \pm 0.4) \times 10^{-5} \text{ s}^{-1}$.

(2) (a) Braichotte, D.; van den Bergh, H. *Appl. Phys. A* 1988, 45, 337. (b) Gilgen, H. H.; Cacouris, T.; Shaw, P. S.; Krohnavek, R. R.; Osgood, R. M. *Appl. Phys. B* 1987, 42, 55. (c) Rand, M. J. *J. Electrochem. Soc.* 1973, 120, 686.

(3) (a) Kumar, R.; Roy, S.; Rashidi, M.; Puddephatt, R. J. *Polyhedron* 1989, 8, 551. (b) Roy, S.; Puddephatt, R. J.; Scott, J. D. *J. Chem. Soc., Dalton Trans.* 1989, 2121.

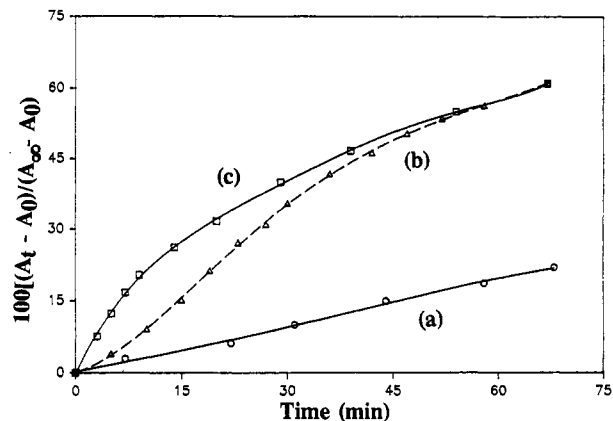


Figure 2. Plot of $100(A_t - A_0)/(A_\infty - A_0)$, where A is the absorbance due to methane, versus time during CVD of platinum from *cis*-[PtMe₂(MeNC)₂] at 250 °C under the following conditions: (a) no preformed Pt film and no H₂ present; (b) no preformed Pt film but H₂ (200 Torr) present; (c) preformed Pt film and H₂ (200 Torr) both present.

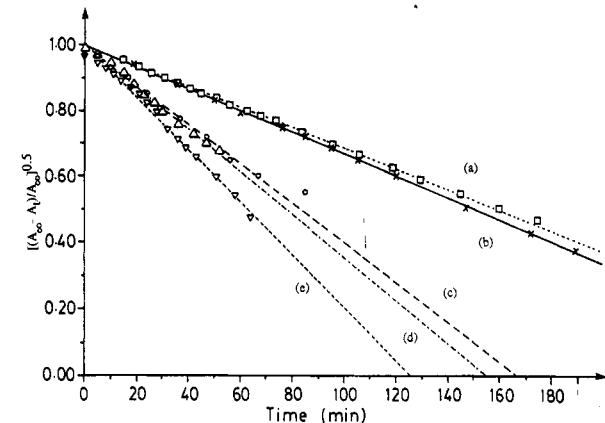


Figure 3. Half-order plots for the decomposition of *cis*-[PtMe₂(MeNC)₂] at 250 °C in the presence of H₂ at the following pressures: (a) 66, (b) 99, (c) 132, (d) 198, (e) 264 Torr.

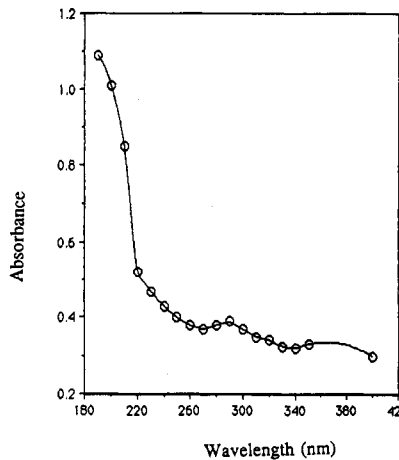


Figure 4. UV-visible absorption spectrum in the gas phase of *cis*-[PtMe₂(MeNC)₂] at 150 °C. The major absorption is centered at 200 nm with a secondary maximum at 290 nm.

(2) The relative rates of thermolysis of 1 and 1', carried out as a mixture of the two complexes with monitoring of both CH₄ and CD₃H formation, gave a secondary isotope effect $k_{\text{H}}/k_{\text{D}} = 1.35 \pm 0.1$.

(3) The reaction was strongly retarded in the presence of free MeNC. Quantitative studies were not possible because MeNC is not thermally stable under the experimental conditions (decay has $t_{1/2} \sim 7 \text{ min}$) but with [1] ca. 1 Torr and [added MeNC]/[1] = 0.54 the initial re-

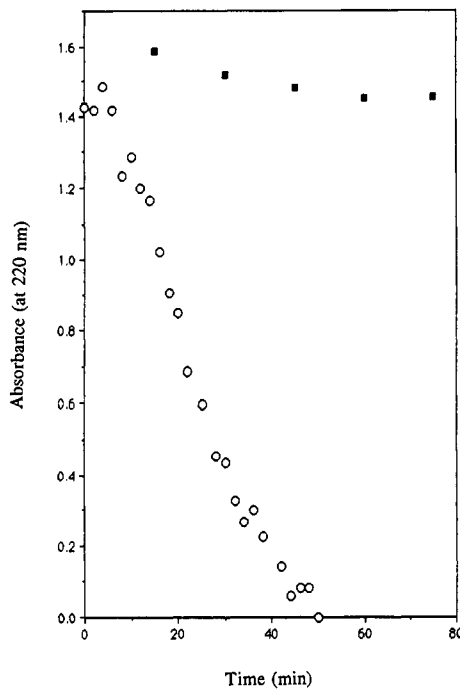


Figure 5. Absorbance due to *cis*-[PtMe₂(MeNC)₂] at 220 nm from a sample under CVD conditions at 150 °C as a function of time. Closed squares, no irradiation except while recording spectra; open circles, with UV irradiation at 220 nm.

tardation is at least a factor of 2.5 and, at higher concentrations of MeNC, CVD was too slow to measure.

(4) The reaction was accelerated in the presence of H₂, but the kinetics became more complex. Typical absorbance vs time plots for methane formation are shown in Figure 2. In the early part of the reaction the order was ~0.5 in complex 1 (Figure 3) and ~0.85 in H₂.

(5) A platinum film was deposited in the central hot zone of the cell by CVD using localizing heating. The cell was then evacuated, fresh precursor was admitted, and the cell was reheated to the CVD temperature by using the standard conditions. CVD occurred more rapidly (Figure 2) and to a major extent on the film whereas, if no pre-formed film was present, platinum was deposited more extensively over the cell walls. This indicates a surface reaction but proof of this is not possible in the present equipment.

Studies of the photochemically enhanced CVD were carried out at 150 °C using a 2-cm pathlength UV cell,

fitted with Suprasil windows, and using the incident UV radiation from a UV-visible spectrophotometer, which was also used to monitor the disappearance of 1. The UV spectrum of 1 is shown in Figure 4, and the decrease in absorbance at 220 nm was used to monitor the reaction. When a Pyrex target was installed, platinum was selectively deposited on the Pyrex surface when illuminated by radiation with $\lambda < 300$ nm. Irradiation at longer wavelengths gave negligible deposition. Figure 5 shows the absorbance vs time plots for CVD in the presence or absence of UV radiation ($\lambda = 220$ nm) at 150 °C. The photochemical enhancement of CVD is immediately obvious since, as seen in Figure 5, thermal CVD at 150 °C is very slow.

In terms of the mechanism of CVD, the strong inhibition by free MeNC strongly suggests a preequilibrium involving reversible dissociation of MeNC from 1 to give *cis*-[PtMe₂(MeNC)], which then undergoes rate-determining thermolysis or hydrogenolysis.⁵ Similar effects have been observed, and similar interpretations made, for the thermolysis of alkylplatinum complexes in solution.^{3b,4} The labeling studies show that the extra hydrogen atom needed to convert a CH₃Pt group to CH₄ is not derived from the second CH₃Pt group but is derived from H₂, if present, or probably from a CH₃NC ligand if H₂ is absent.⁵ The remaining observations and kinetic data strongly indicate a major heterogeneous component to the reaction mechanism.⁶ Further progress requires direct observation of surface bound species in UHV, using IR absorption and thermal desorption methods, and such experiments are in progress.

Acknowledgment. We thank the OCMR and NSERC (Canada) for financial support.

Registry No. 1, 121309-87-3; Pt, 7440-06-4.

(4) To observe first-order kinetics for thermolysis of *cis*-[PtMe₂(MeNC)₂] according to this mechanism, the concentration of free MeNC must be approximately constant. Since MeNC is formed by the thermolysis but then decomposes to involatile products, this is not an unreasonable situation.

(5) The hydrogen could be derived from dissociative adsorption of H₂ or CH₃NC on already-deposited platinum film, for example, or direct hydrogenolysis of PtMe₂(MeNC) could occur. The reaction CH₃ + H₂ → CH₄ + H is endothermic, and so radical formation of methane cannot occur. Isotopic labeling of the MeNC ligand has not been carried out and is necessary to prove the source of the extra hydrogen atom in the methane formed.

(6) (a) Jesinski, J. M.; Meyerson, B. S.; Scott, B. A. *Annu. Rev. Phys. Chem.* 1987, 38, 109. (b) Cole-Hamilton, D. J.; Williams, J. O. *Mechanisms of Reactions of Organometallic Compounds with Surfaces*; Plenum: New York, 1989.